Peierls and Holstein carrier-phonon coupling in crystalline rubrene

Alberto Girlando, Luca Grisanti, and Matteo Masino
Dip. Chimica G.I.A.F., INSTM-UdR Parma, Parma University, I-43124 Parma, Italy

Ivano Bilotti, Aldo Brillante, Raffaele G. Della Valle, and Elisabetta Venuti
Dip. Chim. Fisica ed Inorg., INSTM-UdR Bologna, Bologna University, I-4136 Bologna, Italy
(Received 15 April 2010; revised manuscript received 5 June 2010; published 16 July 2010)

A computational protocol for the calculation of local (Holstein) and nonlocal (Peierls) carrier-phonon coupling in molecular organic semiconductors is presented and applied to orthorhombic rubrene (5,6,11,12-tetraphenyltetracene). In the phonon description, the rigid molecule approximation is removed, allowing mixing of low-frequency intramolecular modes with intermolecular (lattice) phonons. Notwithstanding, a rather clear distinction remains between the low-frequency phonons, which essentially modulate the transfer integral from a molecule to another (Peierls coupling), and the high-frequency, fully intramolecular phonons, which modulate the on-site energy (Holstein coupling). The implications for the current models of mobility are shortly discussed.

DOI: 10.1103/PhysRevB.82.035208 PACS number(s): 81.05.Fb, 72.10.Di

I. INTRODUCTION

In recent years the improvement of chemical purification and crystal growth techniques has led to the production of molecular organic semiconductors with very low structural disorder and intrinsic mobilities on the order of $10-100$ cm^2/V s.[1] These progresses have also spurred intense theoretical research to understand carrier transport in these materials, as both conventional band theory and the Holstein polaron hopping mechanism appear to be inadequate to explain the observed mobilities.[1,2] Several authors have recently pointed out that many features of the organics' mobilities, such as, for instance, the anisotropic temperature dependence, could be accounted for by introducing, in addition to the Holstein coupling, the nonlocal, Peierls-type carrier-phonon coupling.[3–8] The idea can be found also in previous literature[9] but at the time the theories could not be properly tested due to the lack of reliable estimates of the strength of Peierls coupling. Today, more advanced computational methods are available, even though computations at the level of density-functional theory (DFT) are limited to relatively simple molecular crystals such as naphthalene.[3,10,11]

Our group has decided to attack the problem through an experimentally bound semiempirical approach. By this method we can easily calculate the crystal structure and the low-frequency, intermolecular (or lattice) phonons of molecular crystals. Comparison with the experimental Raman spectra validates the computation and, as an additional bonus, allows one to discriminate between different polymorphs of the molecular semiconductor under scrutiny.[12] A first application of the method to calculate the strength of Peierls coupling in pentacene has been published some years ago.[13] Now we apply and perfect the method in calculating and comparing the Peierls and Holstein coupling of a more complex organic semiconductor, rubrene (5,6,11,12-tetraphenyltetracene).

The choice of rubrene has been obviously driven by its importance in the field since it associates one of the highest carrier mobilities among organic semiconductors to interesting optoelectronic properties.[14,15] On the other hand, the rubrene crystal is also a valuable test system for our computational method. The Holstein coupling strength of the isolated molecule has been calculated by DFT methods[16,17] with the intriguing result of a strong coupling by very low-frequency (below 100 cm^{-1}) vibrations. Moreover, Troisi[5] has been able to predict rubrene absolute mobility and its temperature dependence (between 200 and 350 K) by looking at the thermal fluctuations of the transfer integrals. In the model, these fluctuations are connected to Peierls coupling, whose parameters are obtained combining classical molecular dynamics with semiempirical electronic structure calculations.[5] It will be therefore instructive to compare our results with the above, examining how the low-frequency Holstein coupling is modified when the molecule is embedded in the crystal, and at the same time to obtain a more direct and precise analysis of the phonons involved in the Peierls coupling. Our results can also benefit from the numerous experimental investigations on rubrene phonons,[18–20] performed also with reference to the mobility mechanism.[21–23]

II. THEORETICAL METHODOLOGY

In dealing with the complex phonon spectra of molecular crystals, one common approximation is to separate the intramolecular vibrations from the intermolecular, or lattice, phonons. This is the rigid molecule approximation (RMA), in which the lattice phonons correspond to translations and rotations of the rigid molecules. Within the RMA, and in the framework of a molecular orbital (MO) description of the electrons, it is natural to associate the Peierls coupling, i.e., the modulation of intermolecular hopping integrals to lattice phonons. In the same spirit, intramolecular vibrations are expected to modulate only the on-site energies, giving rise to local, or Holstein, carrier-phonon coupling.

However, the isolated rubrene molecule possesses several very low-frequency vibrations[16,18] that inevitably will mix with lattice phonons when the molecules are embedded in the crystal.[19] In addition, computations at the DFT level for

the isolated rubrene molecule predict that about one third of the Holstein coupling strength is associated with low-frequency vibrations.[16] Finally, analogous calculations on the naphthalene crystal have produced the rather unexpected result of a strong Peierls coupling by high-frequency ($\sim$1600 cm^{-1}) intramolecular vibrations.[11] Therefore, we have decided to investigate the consequences of relaxing the RMA on the Peierls coupling, and the relative importance of Peierls and Holstein carrier-phonon coupling, by calculating both contributions for *all* the optical phonons of the rubrene crystal. In the following we shall illustrate the methodology employed to calculate phonon frequencies and eigenvectors, the electronic structure, and the Holstein and Peierls carrier-phonon couplings.

A. Phonon structure

Following a well-assessed treatment,[24] we start by assuming the RMA, and calculate separately the intramolecular and intermolecular vibrations. Intramolecular vibrations are calculated at the DFT level, with the GAUSSIAN03 package,[25] using the B3LYP exchange-correlation functional combined with the 6-31$G(d)$ basis set. As starting molecular geometry we choose that of the molecule within the crystal,[26] adding the constraint of C_{2h} molecular symmetry. The full procedure followed to calculate harmonic frequencies and eigenvectors is described in detail in Ref. 19.

Intermolecular phonon dynamics is calculated by the quasiharmonic lattice-dynamics method.[27,28] In this method the vibrational contribution to the Gibbs energy $G(p,T)$ of the crystal at pressure p and temperature T is approximated by the free energy of the lattice phonons calculated in the harmonic approximation at the average lattice structure:

$$G(p,T) = \Phi_{\text{inter}} + pV + \sum_{\mathbf{k}m} \frac{\hbar\omega_{\mathbf{k}m}}{2} + k_{\text{B}}T \sum_{\mathbf{k}m} \ln\left[1 - \exp\left(-\frac{\hbar\omega_{\mathbf{k}m}}{k_{\text{B}}T}\right)\right]. \quad (1)$$

Here, Φ_{inter} is the intermolecular potential energy of the crystal, pV is the pressure-volume term, $\Sigma_{\mathbf{k}m}\hbar\omega_{\mathbf{k}m}/2$ is the zero-point energy, and the last term is the entropic contribution. The sums are extended to all phonon modes m of wave vector $\mathbf{k}$ and frequency $\omega_{\mathbf{k}m}$. Φ_{inter} is assumed to be described by an atom-atom Buckingham model plus a Coulombic term,

$$\Phi_{\text{inter}} = \frac{1}{2}\sum_{\alpha\beta}\left[A_{\alpha\beta}\exp(-B_{\alpha\beta}r_{\alpha\beta}) - \frac{C_{\alpha\beta}}{r_{\alpha\beta}^6} + \frac{q_\alpha q_\beta}{r_{\alpha\beta}}\right], \quad (2)$$

where the sum is extended to all distances $r_{\alpha\beta}$ between pairs α,β of atoms in *different* molecules considered as rigid bodies, the atoms being fixed at their equilibrium position. The $A_{\alpha\beta},B_{\alpha\beta},C_{\alpha\beta}$ Buckingham parameters involving C and H atoms are from Ref. 29. The charges q_α,q_β in the Coulomb term are the electrostatic-potential-derived atomic charges[25] fitted to the electrostatic potential obtained in the above DFT calculations of the isolated molecule. Given an initial lattice structure, one computes Φ_{inter} and its second derivatives with respect to the displacements of the molecular coordinates. The second derivatives form the dynamical matrix, which is numerically diagonalized to obtain the phonon frequencies $\omega_{\mathbf{k}i}$ and the corresponding eigenvectors. The structure as a function of p and T is then determined self-consistently by minimizing $G(p,T)$ with respect to lattice parameters, molecular positions, and orientations.

At this point we relax the RMA, by introducing the coupling between intramolecular and intermolecular vibrations through the so-called exciton model.[30] The total potential Φ is actually made of intermolecular and intramolecular contributions, Φ_{inter} and Φ_{intra}. In the exciton model, the diagonal derivatives of Φ_{intra} potential are taken to coincide with those of an isolated molecule: $\partial^2\Phi_{\text{intra}}/\partial Q_{ri}^2 = \omega_{ri}^2$. Here ω_{ri} is the frequency of the ith normal mode of the rth molecule. All off-diagonal derivatives are zero, which means no coupling among different normal modes, and no coupling between normal modes and rigid rototranslations. These assumptions are correct by definition for the intramolecular potential at the harmonic level.

The coupling between the molecular and intermolecular coordinates is then introduced perturbatively through Φ_{inter}. Φ_{inter} is described by atom-atom and charge-charge interactions [Eq. (2)], which are both functions only of the interatomic distance. Since the distance depends on the Cartesian coordinates of the atoms, $X_{r\alpha}$, the derivatives of Φ_{inter} can be directly computed in terms of the coordinates $X_{r\alpha}$, and then converted to molecular coordinates Q_{ri},

$$\frac{\partial^2\Phi_{\text{inter}}}{\partial Q_{ri}\,\partial Q_{sj}} = \sum_{\alpha\beta}\frac{\partial^2\Phi_{\text{inter}}}{\partial X_{r\alpha}\,\partial X_{s\beta}}\frac{\partial X_{r\alpha}}{\partial Q_{ri}}\frac{\partial X_{s\beta}}{\partial Q_{sj}}. \quad (3)$$

Here α and β label the Cartesian coordinates of the atoms in molecules r and s, respectively, and the matrix $\partial X_{r\alpha}/\partial Q_{ri}$ describes the Cartesian atomic displacements which correspond to each molecular coordinate Q_{ri}. The displacements corresponding to rigid translations and rotations of the molecules can be derived by simple geometric arguments. The displacements associated to the intramolecular degrees of freedom are the Cartesian eigenvectors of the normal modes of the isolated molecule. The displacements, together with the intermolecular potential model, determine the coupling between intramolecular and intermolecular modes. We remark that the intramolecular degrees of freedom are taken into account only as far as their effects on the vibrational contribution to the free energy are concerned. No attempt to decrease the potential energy by deforming the molecules is made.

B. Electronic structure

Holstein and Peierls coupling are connected to the modulation by the phonons of on-site energies ϵ_r and the transfer integrals t_{rs}, respectively, which within the tight binding, MO approximation are given by

$$\epsilon_r = \langle\varphi_r|\mathbf{H}|\varphi_r\rangle, \quad (4)$$

$$t_{rs} = \langle\varphi_r|\mathbf{H}|\varphi_s\rangle, \quad (5)$$

where $\mathbf{H}$ is the one-particle electronic Hamiltonian, and φ_r and φ_s are the highest-occupied MO (HOMO) or lowest-

unoccupied MO (LUMO), for hole or electron transport, respectively, of the molecules at sites r and s. Calculating the modulation of these quantities by all the phonons in the rubrene crystal is exceedingly onerous, so we have chosen a semiempirical approach based on the INDO (intermediate neglect of differential overlap) Hamiltonian with the Zerner spectroscopic parametrization (INDO/S).[31,32]

While the HOMO, LUMO energies ϵ_r are directly given by the INDO/S method for the rubrene molecule, the calculation of the transfer integral between two molecules (a dimer) requires some comment. One common approach is the so-called "energy splitting in the dimer" (ESD) model. The ESD model considers the energy splitting of the two HOMO (or LUMO) orbitals in the dimer with respect to the isolated molecule. The energy separation between the HOMO-1 and HOMO (LUMO and LUMO+1) of the dimer is then taken to be twice the transfer integrals between the two molecules,

$$\Delta\epsilon = 2|t_{rs}|. \tag{6}$$

This approach cannot determine the sign of t, which instead is important when considering the t's of different dimers within the crystal. Moreover, the approach is valid only for exactly equivalent molecules, which have to remain equivalent also during a vibration. The latter condition is clearly inapplicable for nontotally symmetric modes.[5]

We therefore consider directly the interacting matrix element between the frontier orbitals of the two molecules r and s within the dimer. We first perform the calculation for the two isolated molecules $i=r,s$,

$$\mathbf{f}^i\varphi_i^0 = \epsilon_i\varphi_i^0, \tag{7}$$

where $\mathbf{f}^i$ is the Fock operator for each molecule in the dimer and φ_i^0 the corresponding HOMO or LUMO with energy ϵ_i. Next we repeat the calculation for the full dimer,

$$\mathbf{f}^{rs}\varphi_{rs} = \epsilon_{rs}\varphi_{rs}. \tag{8}$$

The transfer integral is then given by

$$t_{rs} = \langle\varphi_r^0|\mathbf{f}^{rs}|\varphi_s^0\rangle. \tag{9}$$

In the INDO/S method φ_r and φ_s are expressed as linear combinations of atomic orbitals (AOs) χ_λ and χ_μ,

$$\varphi_r^0 = \sum_\lambda c_{r\lambda}\chi_\lambda \quad \varphi_s^0 = \sum_\mu c_{s\mu}\chi_\mu. \tag{10}$$

Equation (9) can then be rewritten as

$$t_{rs} = \sum_\lambda \sum_\mu c_{r\lambda}c_{s\mu}\langle\chi_\lambda|\mathbf{f}^{rs}|\chi_\mu\rangle, \tag{11}$$

where the $\langle\chi_\lambda|\mathbf{f}^{rs}|\chi_\mu\rangle$ is the Fock matrix element on the dimer AO basis. The above equation is easily implemented in the INDO/S program.[32]

C. Carrier-phonon coupling

The strength of carrier-phonon coupling can be expressed in a variety of ways and computed by different methods.[2] Here we shall follow the nomenclature and procedure adopted by our laboratory since its studies on electron-phonon coupling in organic charge-transfer crystals.[24,33]

We define the linear Holstein and Peierls coupling constants as follows:

$$g_{\mathrm{H}}(r;\mathbf{k}m) = \left(\frac{\partial\epsilon_r}{\partial q_{\mathbf{k}m}}\right) = \sqrt{\frac{\hbar}{2\omega_{\mathbf{k}m}}}\left(\frac{\partial\epsilon_r}{\partial Q_{\mathbf{k}m}}\right), \tag{12}$$

$$g_{\mathrm{P}}(rs;\mathbf{k}m) = \left(\frac{\partial t_{rs}}{\partial q_{\mathbf{k}m}}\right) = \sqrt{\frac{\hbar}{2\omega_{\mathbf{k}m}}}\left(\frac{\partial t_{rs}}{\partial Q_{\mathbf{k}m}}\right), \tag{13}$$

where, as defined above, ϵ_r is the HOMO or LUMO energy of the molecule at site r and t_{rs} is the transfer integral between the HOMOs or the LUMOs of two molecules r and s. Moreover, $q_{\mathbf{k}m}$ and $Q_{\mathbf{k}m}$ are, respectively, the dimensionless and dimensional (spectroscopic) normal coordinate of mode m of wave vector $\mathbf{k}$ and frequency $\omega_{\mathbf{k}m}$. With this definition, both g's are expressed in energy units, at variance with other current definitions.[2]

In the following we shall make the approximation of considering the only optical ($\mathbf{k}=0$) phonons with the reasonable assumption that the coupling constants do not vary considerably with $\mathbf{k}$. Consistently with this approximation, we disregard the coupling to acoustic phonons, although the coupling at the zone edges may be of the same order of magnitude as that of the optical phonons.[34] Therefore we shall henceforth drop the index $\mathbf{k}$. Since we are dealing with a set of equal molecules, we can also drop the index r. We shall also report only the results for the HOMOs (valence band), the only ones relevant to the experimental hole mobility of rubrene.

The strength of the Holstein and Peierls coupling is expressed by the small polaron binding energy, ϵ_{sp}, and by the lattice distortion energy, ϵ_{d}, respectively, defined as[24,33]

$$\epsilon_{\mathrm{sp}} = \sum_m \epsilon_{\mathrm{sp}}(m) = \sum_m g_{\mathrm{H}}^2(m)/\omega_m, \tag{14}$$

$$\epsilon_{\mathrm{d}} = \sum_{mt} \epsilon_{\mathrm{d}}(t;m) = \sum_{mt} g_{\mathrm{P}}^2(t)/\omega_m, \tag{15}$$

where the summations run over all the optical modes m of the crystal (both intramolecular and intermolecular) and over all the nonequivalent transfer integrals t. If one assumes that the normal modes of the neutral and ionized molecule are equal, a reasonable assumption when considering all the modes together, the small polaron binding energy ϵ_{sp} is one half of λ, the reorganization energy.[2]

III. RESULTS

The most commonly encountered rubrene phase is orthorhombic, space group $Cmca$ (D_{2h}^{18}) with four molecules per unit cell.[19,26] The conventional cell is nonprimitive (C face centered) with two molecules exchanged by a rototranslation and two more molecules obtained by a nonprimitive translation. The primitive unit cell contains two molecules, which have C_{2h} symmetry and lie on sites with symmetry $2/m$. The uncommonly high symmetry of the rubrene crystal simplifies the problem, as many quantities are zero by symmetry or have equal absolute values.

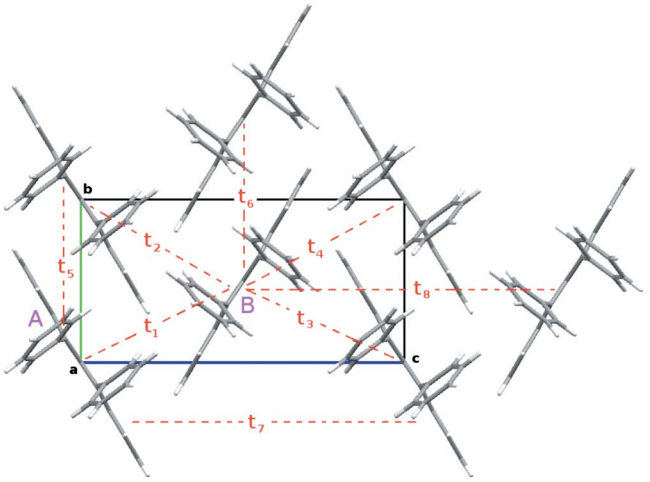

FIG. 1. (Color online) Crystal structure of orthorhombic rubrene. The two independent molecules (A and B) within the primitive cell and the eight nearest-neighbor transfer integrals are evidenced.

Figure 1 shows the crystal structure of orthorhombic rubrene. A and B label the two independent molecules within the primitive unit cell and t_1 to t_8 indicate the nearest-neighbor transfer integrals. The transfer integrals t_1 to t_4 are all equal by symmetry. The same applies to t_5 and t_6 integrals, and to t_7 and t_8. INDO/S values for the HOMO t's are: t_{1-4}=−0.006 eV, $t_{5,6}$=0.125 eV, and $t_{7,8}$=0.000 eV. The value of $t_{5,6}$ is in agreement with previous estimates,[5,16,17] whereas that of t_{1-4} is somewhat lower.[5] In any case, the electronic structure of orthorhombic rubrene is anisotropic with the hopping probability mainly directed along the b crystal axis.

We first analyze the Holstein coupling g_{H}. For the isolated molecule, only totally symmetric molecular modes (a_g) can have g_{H} different from zero. The top of Fig. 2 reports the small polaron binding energies, $\epsilon_{\mathrm{sp}}(m)$, for each mode in the isolated molecule, as calculated for the rubrene HOMOs by

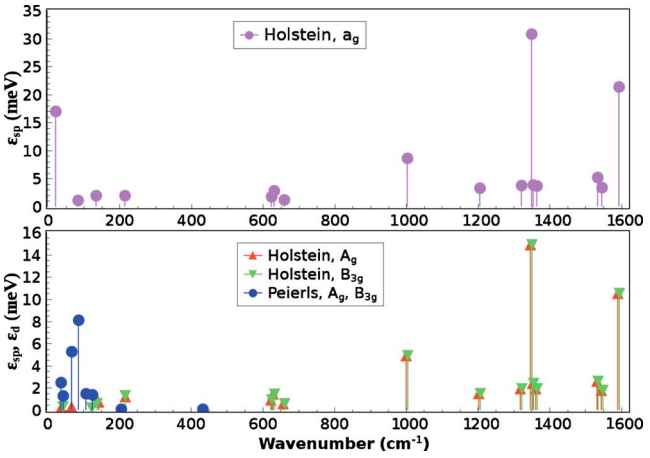

FIG. 2. (Color online) Top panel: single-mode small polaron binding energy in isolated rubrene molecule. Bottom panel: single-mode small polaron binding energy (red and green lines) and lattice distortion energy (blue lines) of rubrene crystal. Notice the different energy scale in the two panels.

TABLE I. Holstein and Peierls coupling constants of low-frequency (10–250 cm^{-1}) phonons in the orthorhombic rubrene crystal. Frequencies ($\bar{\nu}$) in reciprocal centimeter and coupling constants in millielectron volt. The observed frequencies are from Ref. 19.

	$\bar{\nu}$ calc.	% intra	$\bar{\nu}$ obs.	g_{H}	g_{P}
A_g	37.4	46.8	35.5	−0.9	3.4
	66.6	78.5	75.3	1.6	−6.6
	106.3	81.1	104.8	0	−4.4
	125.1	94.5	118.6	1.4	−4.7
	142.6	99.2	139.6	0	0
	217.7	100.0	220.2	−5.7	1.1
B_{3g}	43.1	61.2	35.5	1.3	−2.6
	86.7	48.4	75.3	−0.6	−9.3
	90.6	95.7	87.4	0.1	0.4
	123.9	96.1	104.0	1.7	−1.1
	138.2	98.7	139.2	3.3	−1.3
	216.8	100.0		−5.8	1.0

the INDO/S method. The $\epsilon_{\mathrm{sp}}(m)$'s are somewhat higher than those calculated by DFT methods,[16,17] but the *relative* values show the same trend, the highest values being relevant to the modes at 1594, 1349, 1002, and 21 cm^{-1}. The INDO/S total small polaron binding energy is 112 meV, to be compared with the DFT values of 80 meV and 75 meV in Refs. 16 and 17, respectively.

When the molecule is embedded in the crystal, the a_g modes of the two molecules in the primitive unit cell couple in phase and out of phase, yielding phonons of A_g and B_{3g} crystalline symmetry, respectively.[19] In addition, we have the lattice phonons, which mix with the low-frequency molecular phonons (Table I). The single-mode small polaron binding energies are reported in the bottom panel of Fig. 2, red and green lines. The comparison between the top and bottom panels of the figure immediately shows that the Holstein coupling strength of the lowest frequency a_g molecular mode, at 21 cm^{-1}, is essentially washed out when the molecule is embedded in the crystal. Due to the mixing with the lattice modes, the coupling strength of the mode is indeed distributed over several phonons. In addition, the packing inside the crystal makes the molecule more rigid (higher frequencies of the modes), again contributing to the reduction in the coupling strength. The calculated total small polaron binding energy of the rubrene molecule in the crystal is 99 meV, slightly smaller than that for the isolated molecule. The numerical values of the coupling constants are reported in the fifth column of Table I for the low-frequency modes, and in the second and fifth columns of Table II, for the high-frequency, fully intramolecular modes. Clearly, the coupling of the high-frequency modes dominates, the strongest coupling being associated to the 1594, 1349, and 1002 cm^{-1} phonons (Fig. 3), which account for about 60% of the total coupling strength.

We now turn our attention to the Peierls coupling. A simple symmetry analysis indicates that phonons belonging

TABLE II. A_g and B_{3g} Holstein and Peierls coupling constants of pure intramolecular modes in the orthorhombic rubrene crystal. Frequencies ($\bar{\nu}$) in reciprocal centimeter and coupling constants in millielectron volt. Only modes with $g_H \geq 5.0$ meV or with $g_P \geq 1.0$ meV are reported. A_g and B_{3g} modes have the same frequency and coupling constants, so only a single value is shown.

$\bar{\nu}$ calc.	g_H	g_P	$\bar{\nu}$ calc.	g_H	g_P
450.2	0	2.6	1205.3	−15.1	0
624.5	8.22	0	1233.4	5.0	0
631.2	−10.8	1.3	1321.4	−17.5	0
659.1	−7.2	0	1348.6	49.9	0
672.4	0	1.7	1354.5	20.1	0
781.6	0	1.4	1363.6	−17.8	0
909.5	7.0	0	1487.0	5.2	0
924.1	−5.3	0	1536.3	22.4	0
989.6	6.5	0	1546.3	18.6	0
1002.3	24.6	0	1593.8	−45.6	1.6
1018.5	6.8	0	1658.1	5.6	0

to the B_{1g}, B_{2g}, A_u, and B_{3u} crystal symmetry species cannot modulate the transfer integrals. The B_{1u} and B_{2u} phonons modulate the t_{1-4} integrals, but the coupling in negligibly small (less than 1 meV), since the integrals themselves are small. The A_g and B_{3g} phonons can couple both to the t_{1-4} and to the $t_{5,6}$ transfer integrals but only the latter are appreciably different from zero. The sign of $g_P(5;l)$ and $g_P(6;l)$ is the same for the A_g phonons and opposite for the B_{3g} ones. The values of the Peierls coupling constants relevant to t_5 are reported in the sixth column of Table I and in the third and sixth columns of Table II. The lattice distortion energy of the individual phonons is compared with the corresponding small polaron binding energy in the bottom panel of Fig. 2.

From Tables I and II and Fig. 2 it is immediately evident that only the low-frequency phonons exhibiting some component of intermolecular displacement are able to appreciably modulate the transfer integrals. The most strongly coupled phonons are the second lowest frequency of each symmetry species, namely, the A_g mode at 66.6 cm^{-1} and the B_{3g} mode at 86.7 cm^{-1}. Among the fully intramolecular vibrations, only the modes at 450.2, 631.2, 672.4, 781.6, and 1693.8 cm^{-1} show weak coupling to the transfer integrals, but given their high frequency they yield negligible contribution to ϵ_d. The total lattice distortion energy is calculated to be about 20 meV.

Despite the mixing between intramolecular and intermolecular modes, particularly strong in rubrene due to the presence of the heavy phenyl groups, a rather sharp separation persists between Holstein and Peierls coupled phonons. The former are indeed high-frequency, fully intramolecular modes, and the latter are low-frequency modes, with clear intermolecular character (Fig. 2, bottom). Very few phonons exhibit both types of coupling (Tables I and II), and in general one of the coupling dominates on the other.

Figure 3 pictorially reports the eigenvectors of the three most strongly coupled Holstein modes. All three imply CC stretching vibrations of the tetracene skeleton, as it might have been expected since the HOMO is mostly localized on the tetracene rings. Only the 1002 cm^{-1} mode presents some contribution of the ring breathing of the phenyl groups but the modulation of the HOMO energy is in any case bound to the vibrations of the tetracene.

The eigenvectors of the four most strongly coupled Peierls modes are reported in Fig. 4. The A_g and B_{3g} modes at 67 and 87 cm^{-1} are rather similar, both implying the relative displacements of the tetracene skeletons of the molecules aligned along the b axis. On the other hand, the A_g modes at 37 cm^{-1} and at 106, and the pair of A_g and B_{3g} phonons around 120 cm^{-1} (the latter not reported in the figure) mostly involve the lateral phenyl group. A more detailed analysis of the eigenvectors shows that the lowest frequency a_g mode of the isolated molecule, calculated at 20 cm^{-1} (top of Fig. 2), in the crystal redistributes mainly over four phonons, A_g at 37.4 and 66.6 cm^{-1}, and B_{3g} at 43.1 and 86.7 cm^{-1}.

IV. DISCUSSION

We have obtained a detailed description of the phonons in crystalline rubrene, and of their local and nonlocal coupling with the holes in the valence band. Of course, we cannot give strict confidence to the obtained absolute values of the coupling constants but we can certainly assess the relative mag-

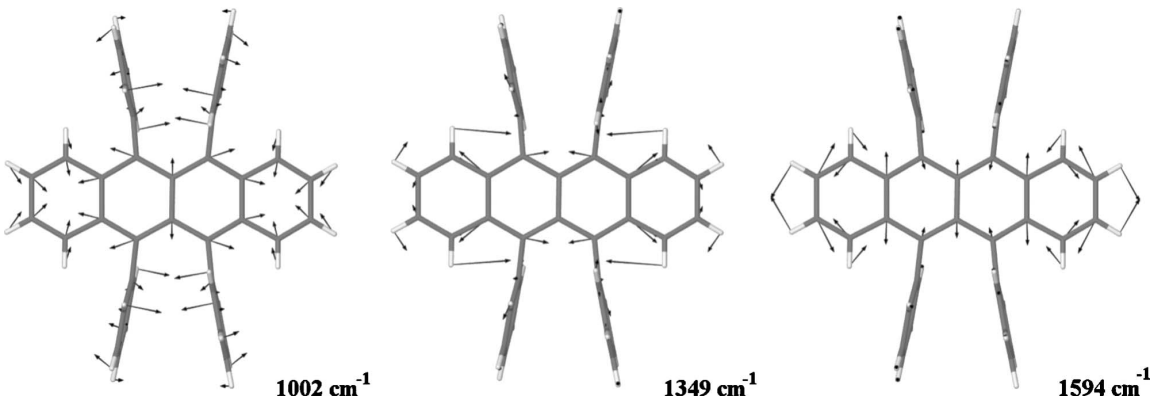

FIG. 3. The three most strongly coupled Holstein phonons.

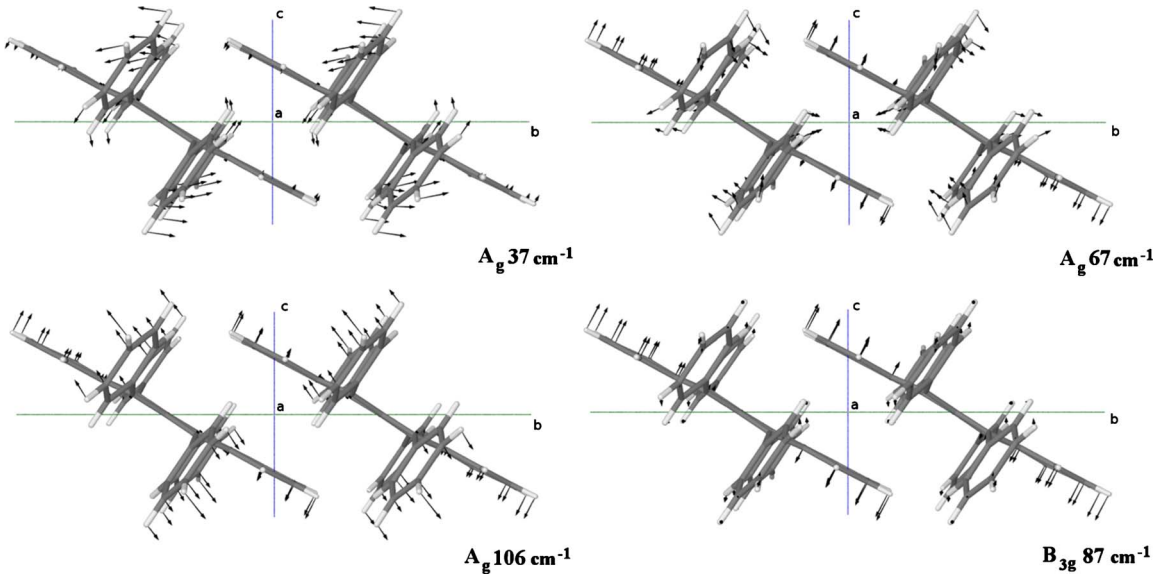

FIG. 4. (Color online) Four examples of strongly coupled Peierls phonons.

nitude of Holstein and Peierls coupling strengths. Indeed, having adopted a unified method of calculation, and having also taken into account the change in the phonon description when the rubrene molecule is embedded into the crystal, we can confidently state that the overall coupling strength of the Peierls coupling (ϵ_d) is about one fifth of the strength of the Holstein coupling (ϵ_{sp}).

We now address the connection of the present results with the issue of rubrene mobility. As mentioned in Sec. I, the high-temperature (200–350 K) mobility of rubrene has been rather accurately predicted by Troisi in terms of the time-dependent fluctuations of the transfer integrals, obtained by classical molecular dynamics and INDO/S.[5] The approach is in many aspect complementary to ours, so it is instructive to compare the corresponding results.

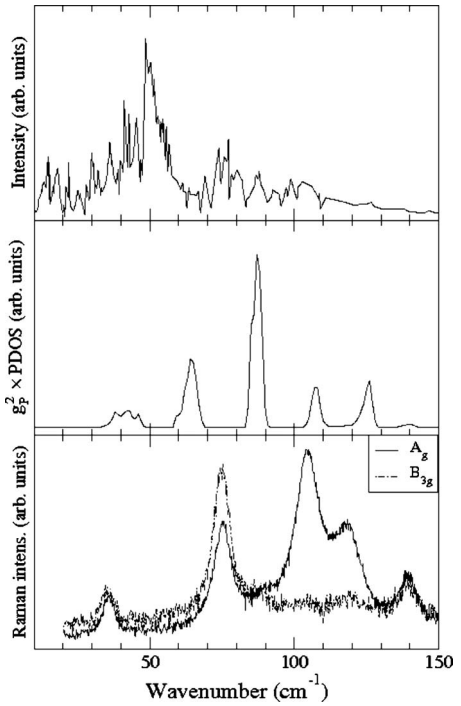

FIG. 5. Top panel: frequency analysis of the nuclear motions that modulate more strongly the transfer integral along the *b* axis (adapted from Ref. 5). Middle panel: Peierls coupling constant multiplied by the PDOS. Bottom panel: Raman spectrum reporting the A_g and B_{3g} phonons (adapted from Fig. 1 of Ref. 19).

The top of Fig. 5 reports the Fourier transform of the autocorrelation function of the time-dependent transfer integrals along the rubrene *b* axis, adapted from Ref. 5. The peaks correspond to frequencies of the phonons that most strongly modulate the transfer integrals, namely, that have the strongest Peierls coupling constants. In the middle panel we plot what can be considered as the analogous function in the framework of our method, namely, the squares of the Peierls coupling constants (Table I) multiplied by the relevant phonon density of states (PDOS). It is seen that our function is more strongly peaked than that obtained by Troisi[5] due to the relatively small dispersion of the implied phonons. The latter point justifies our assumption of disregarding the wave-vector dependence of the coupling constants (cf. Sec. II C). In addition, the Troisi's function is peaked around 50 cm^{-1}, whereas in our case the majors peaks occur at higher frequencies, in good agreement with the experimental A_g and B_{3g} Raman frequencies, reported in the lowest panel of Fig. 5 (adapted from Ref. 19). On the other hand, the mobility does not depend on the details of the carrier phonons coupling. As a matter of fact, in the Troisi's model the mobility is computed on the basis of only one effective phonon per type (Holstein and Peierls) with coupling strength taken as twice ϵ_{sp} and ϵ_d. The effective phonons frequency is roughly set equal to the frequency of the most strongly coupled mode.[5]

Our calculated total Holstein and Peierls coupling strengths (99 meV and 20 meV, respectively) have the same ratio as the reorganization energies used in Ref. 5. For the frequency of the effective phonons, we use the weighted average of the coupled frequencies,[35]

$$\omega_{\text{eff}} = \frac{\sum_j \omega_j \epsilon_j}{\sum_j \epsilon_j}, \tag{16}$$

where ω_j are the frequencies of either the Holstein or Peierls coupled modes with small polaron binding energy or lattice distortion energy ϵ_j. We obtain an effective frequency of 1277 cm^{-1} and 77 cm^{-1} for the Holstein and Peierls coupled modes, respectively, to be compared with the 1400 and 50 cm^{-1} values adopted in Ref. 5. Then two different approaches give comparable parameters in terms of which the rubrene mobility around room temperature is satisfactorily reproduced. This finding reinforces the idea that the model of transfer integral fluctuations is able to account for the mobility mechanism in organic semiconductors.

One distinctive feature of rubrene mobility is its fast drop below about 170 K.[15] This sharp decrease has been attributed to carrier trapping[15] or to the enhancement of the carriers effective mass.[22] More recently, it has been noted that a significant decrease in width of several low-frequency Raman bands occur between 200 and 150 K.[20] This finding has brought the authors to propose a model by which the sharp mobility decrease is associated to a decreased conformational disorder in the lateral phenyl groups. The idea is interesting, but we should remark that not all the low-frequency modes imply oscillations of the phenyl groups (see Fig. 4), and that in general the bandwidth decrease in low-frequency phonons is also connected with the decrease in excited states population with temperature. A more detailed study of the Raman bandwidth decrease, possibly with polarized light on single crystals,[19] might help in clarifying the matter.

One last point we wish to address is the appearance of an infrared (IR) band around 500 cm^{-1} on operating devices[21,22] or on photoexcitation,[23] namely, in the presence of charge carriers. It is tempting to attribute this band to a phenomenon analogous to that observed in polyacetylene or other conducting polymers. In these systems, in fact, doping or photoexcitation induces strong IR absorptions in correspondence with Peierls coupled modes, due to symmetry breaking induced by the charges.[36,37] As we have seen before, rubrene electronic structures has a quasi-one-dimensional character along *b*, although the corresponding bandwidth (~0.5 eV) is about 20 times smaller than the bandwidth of, e.g., polyacetylene (~10 eV). Table II shows that in the frequency range 450–750 cm^{-1} some intramolecular modes display Peierls coupling. The coupling is rather weak, however. The connection of the rubrene ~500 cm^{-1} IR band with the phenomena observed in conducting polymers indeed requires confirmation by further IR investigations, notably in the spectral region where most of the Peierls coupled modes occur, below 150 cm^{-1} (Table I).

V. CONCLUSIONS

In this paper we have proposed a computational protocol for the calculation of local (Holstein) and nonlocal (Peierls) carrier-phonon coupling in molecular organic semiconductors. The two types of coupling are computed by the same method, allowing a reliable assessment of the relative coupling strength. The approach is semiempirical so that it can be easily applied to complex molecular crystals such as rubrene. The results of the calculations are validated by the comparison with experiment (Raman spectra) and by partial results obtained by other computational approaches. One key ingredient of our method is to allow interaction and mixing of the intermolecular and intramolecular phonons. The mixing is fundamental in accounting for the phonon related properties of the crystal at hand.[34]

Due to the presence of heavy lateral phenyl group, isolated (gas phase) rubrene has several low-frequencies vibrations, some of which show strong Holstein coupling to the charge carrier.[16,17] However, we have put in evidence that embedding the rubrene molecule in the crystal strongly attenuate the Holstein coupling of low-frequency phonons. Actually, the overall Holstein coupling strength is slightly decreased in the crystal. Calculation of both Holstein and Peierls coupling constants for *all* the phonons in the rubrene crystal shows that despite the mixing between intermolecular and intramolecular phonons, a rather clear separation remains between the low-frequency phonons, which mostly modulate the transfer integral, and the high-frequency phonons modulating the on-site energies (Fig. 2).

There are of course several approximations in our calculations, for instance, we calculate the coupling constants only for the optical phonons at the zone center. In addition, we disregard the anharmonicity, which in the case of low-frequency phonons might have important effects on the physical properties above 100–150 K. On the other hand, macroscopic properties such as the mobility do not depend strongly from the details of the carrier-phonon coupling. Indeed, models aimed at reproducing the temperature dependence of the mobility of organic semiconductors use single effective phonons as model parameters.[5,8] The effective phonon frequency and coupling strength we have calculated for rubrene agree nicely with those independently adopted by Troisi in accounting for the room-temperature rubrene mobility.[5] This finding gives support to the proposed mobility mechanism. However, we believe that we can start trusting a model once it is able to explain the differences in the mobility of different systems. The computational protocol presented in this paper can easily provide parameters for the local and nonlocal carrier-phonon coupling in other organic semiconductors, then validating models for the mobility mechanism.

[1] M. E. Gershenson, V. Podzorov, and A. F. Morpurgo, Rev. Mod. Phys. **78**, 973 (2006).
[2] V. Coropceanu, J. Cornil, D. A. da Silva Filho, Y. Olivier, R. Silbey, and J. L. Brédas, Chem. Rev. **107**, 926 (2007).
[3] K. Hannewald and P. A. Bobbert, Appl. Phys. Lett. **85**, 1535 (2004).
[4] A. Troisi and G. Orlandi, Phys. Rev. Lett. **96**, 086601 (2006).
[5] A. Troisi, Adv. Mater. **19**, 2000 (2007).
[6] J.-D. Picon, M. N. Bussac, and L. Zuppiroli, Phys. Rev. B **75**, 235106 (2007).
[7] J. J. Kwiatkowski, J. M. Frost, J. Kirkpatrick, and J. J. Nelson, J. Phys. Chem. A **112**, 9113 (2008).
[8] S. Fratini and S. Ciuchi, Phys. Rev. Lett. **103**, 266601 (2009).
[9] E. A. Silinsh and V. Čápek, *Organic Molecular Crystals: Interaction, Localization, and Transport Phenomena* (AIP, New York, 1994).
[10] L. J. Wang, Q. Peng, Q. K. Li, and Z. Shuai, J. Chem. Phys. **127**, 044506 (2007).
[11] V. Coropceanu, R. Sánchez-Carrera, P. Paramonov, G. M. Day, and J. L. Brédas, J. Phys. Chem. C **113**, 4679 (2009).
[12] A. Brillante, I. Bilotti, R. G. Della Valle, E. Venuti, and A. Girlando, CrystEngComm **10**, 937 (2008).
[13] R. G. Della Valle, A. Brillante, L. Farina, E. Venuti, M. Masino, and A. Girlando, Mol. Cryst. Liq. Cryst. **416**, 145 (2004).
[14] V. C. Sundar, J. Zaumseil, V. Pozdorov, E. Menard, R. Willett, T. Someya, M. Gershenson, and J. A. Rogers, Science **303**, 1644 (2004).
[15] V. Podzorov, E. Menard, A. Borissov, V. Kiryukhin, J. A. Rogers, and M. E. Gershenson, Phys. Rev. Lett. **93**, 086602 (2004).
[16] D. A. da Silva Filho, E.-G. Kim, and J. L. Brédas, Adv. Mater. **17**, 1072 (2005).
[17] G. Nan, X. Yang, L. Wang, Z. Shuai, and Y. Zhao, Phys. Rev. B **79**, 115203 (2009).
[18] J. R. Weinberg-Wolf, L. E. McNeil, S. Liu, and C. Kloc, J. Phys.: Condens. Matter **19**, 276204 (2007).
[19] E. Venuti, I. Bilotti, R. G. Della Valle, A. Brillante, P. Ranzieri, M. Masino, and A. Girlando, J. Phys. Chem. C **112**, 17416 (2008).
[20] Z. Q. Ren, L. E. McNeil, S. Liu, and C. Kloc, Phys. Rev. B **80**, 245211 (2009).
[21] M. Fischer, M. Dressel, B. Gompf, A. K. Tripathi, and J. Pflaum, Appl. Phys. Lett. **89**, 182103 (2006).
[22] Z. Q. Li, V. Podzorov, N. Sai, M. C. Martin, M. E. Gershenson, M. Di Ventra, and D. N. Basov, Phys. Rev. Lett. **99**, 016403 (2007).
[23] M. Koeberg, E. Hendry, J. M. Schins, H. A. van Laarhoven, C. F. J. Flipse, K. Reimann, M. Woerner, T. Elsaesser, and M. Bonn, Phys. Rev. B **75**, 195216 (2007).
[24] A. Girlando, M. Masino, G. Visentini, R. G. Della Valle, A. Brillante, and E. Venuti, Phys. Rev. B **62**, 14476 (2000).
[25] M. J. Frisch, G. W. Trucks, H. B. Schlegel, G. E. Scuseria, M. A. Robb, J. R. Cheeseman, J. A. Montgomery, Jr., T. Vreven, K. N. Kudin, J. C. Burant, J. M. Millam, S. S. Iyengar, J. Tomasi, V. Barone, B. Mennucci, M. Cossi, G. Scalmani, N. Rega, G. A. Petersson, H. Nakatsuji, M. Hada, M. Ehara, K. Toyota, R. Fukuda, J. Hasegawa, M. Ishida, T. Nakajima, Y. Honda, O. Kitao, H. Nakai, M. Klene, X. Li, J. E. Knox, H. P. Hratchian, J. B. Cross, V. Bakken, C. Adamo, J. Jaramillo, R. Gomperts, R. E. Stratmann, O. Yazyev, A. J. Austin, R. Cammi, C. Pomelli, J. W. Ochterski, P. Y. Ayala, K. Morokuma, G. A. Voth, P. Salvador, J. J. Dannenberg, V. G. Zakrzewski, S. Dapprich, A. D. Daniels, M. C. Strain, O. Farkas, D. K. Malick, A. D. Rabuck, K. Raghavachari, J. B. Foresman, J. V. Ortiz, Q. Cui, A. G. Baboul, S. Clifford, J. Cioslowski, B. B. Stefanov, G. Liu, A. Liashenko, P. Piskorz, I. Komaromi, R. L. Martin, D. J. Fox, T. Keith, M. A. Al-Laham, C. Y. Peng, A. Nanayakkara, M. Challacombe, P. M. W. Gill, B. Johnson, W. Chen, M. W. Wong, C. Gonzalez, and J. A. Pople, GAUSSIAN03, Revision D.02, Gaussian Inc., Wallingford, CT, 2004.
[26] O. D. Jurchescu, A. Meetsma, and T. T. M. Palstra, Acta Crystallogr., Sect. B: Struct. Sci. **62**, 330 (2006).
[27] W. Ludwig, *Recent Developments in Lattice Theory, Springer Tracts in Modern Physics* (Springer-Verlag, Berlin, 1967), Vol. 43.
[28] R. G. Della Valle and E. Venuti, Phys. Rev. B **58**, 206 (1998).
[29] D. E. Williams, J. Mol. Struct. **485-486**, 321 (1999).
[30] S. Califano, V. Schettino, and N. Neto, *Lattice Dynamics of Molecular Crystals* (Springer-Verlag, Berlin, 1981).
[31] J. Ridley and M. Zerner, Theor. Chim. Acta **32**, 111 (1973); **42**, 223 (1976).
[32] Since the original INDO/S (ZINDO) code is not in the public domain, we have updated and modified the code from the CINDO QCPE program described in J. A. Pople and D. L. Beveridge, *Approximate Molecular Orbital Theory* (McGraw-Hill, New York, 1970). The parametrization has been taken from the original papers by the Zerner group (Ref. 31) and checked against those found in the ARGUSLAB program files, ARGUSLAB free package: http://www.arguslab.com/
[33] A. Painelli and A. Girlando, J. Chem. Phys. **84**, 5655 (1986). Notice a misprint in footnote 24, which should read $q_R = Q\sqrt{2\omega/\hbar}$.
[34] A. Girlando, M. Masino, A. Brillante, R. G. Della Valle, and E. Venuti, Phys. Rev. B **66**, 100507(R) (2002).
[35] A. Girlando, M. Masino, A. Painelli, N. Drichko, M. Dressel, A. Brillante, R. G. Della Valle, and E. Venuti, Phys. Rev. B **78**, 045103 (2008).
[36] J. Orenstein, in *Handbook of Conducting Polymers*, edited by T. A. Skotheim (M. Dekker, New York, 1988), Vol. 2, p. 1297, and references therein.
[37] Z. G. Soos, D. Mukhopadhyay, A. Painelli, and A. Girlando, in *Handbook of Conducting Polymers*, 2nd ed., edited by T. A. Skotheim, R. L. Elsenbaumer, and J. R. Reynolds (Dekker, New York, 1998), p. 165.